

## Supporting information

### Top and bottom electrode optimization enabled high-performance flexible and semi-transparent organic solar cells

Yuheng Wang,<sup>a,b</sup> Guodong Wang,<sup>b</sup> Yi Xing,<sup>b</sup> Muhammad Abdullah Adil,<sup>b</sup> Waqar Ali Memon,<sup>b</sup> Yilin Chang,<sup>b</sup> Lixuan Liu,<sup>b</sup> Chen Yang,<sup>b</sup> Meng Zhang,<sup>a</sup> Dongfan Li,<sup>a</sup> Jianqi Zhang,<sup>\*,b</sup> Guanghao Lu,<sup>\*,a</sup> Zhixiang Wei<sup>\*,b,c</sup>

<sup>a</sup>Frontier Institute of Science and Technology, Xi'an Jiaotong University, Xi'an, 710054, China;

<sup>b</sup>CAS Key Laboratory of Nanosystem and Hierarchical Fabrication, CAS Center for excellence in Nanoscience, National Center for Nanoscience and Technology, Beijing 100190, China;

<sup>c</sup>University of Chinese Academy of Sciences, Beijing, 100049, China

**Table S1** The comparable summary of large-area / semi-transparent devices.

Systems	Area (cm <sup>2</sup> )	PCE (%)	AVT (%)	Top electrode	Ref
<b>PM6:ID-4CI</b>	1	1.11	44	UTMF	1
<b>PBTZT-stat-BDTT-8: 4TICO</b>	1.1	3.9	30	PH1000	2
<b>PTB7-Th: PC<sub>71</sub>BM</b>	4	6.93	11.5	With Grids	3
<b>PffBT4T-2OD: PC<sub>61</sub>BM:PC<sub>71</sub>BM</b>	1.1	5.8	6	PEDOT:PSS	4
<b>PBDTT-F-TT: PC<sub>71</sub>BM</b>	1	6.44	-	UTMF	5
		7.21		Cross Grids	
		6.57		Double Cross Grids	
		6.67	21.36	15 nm UTMF	
<b>PTB7-Th: Coi8DFIC: PC<sub>61</sub>BM</b>	1.25	7.74	18.27	UTMF + Busbar 1	This Work
		8.06	15.84	UTMF + Busbar 2	

**Table S2** Basic efficiency statistics of mainstream semitransparent systems, all are small-area (0.04 cm<sup>2</sup>) rigid device efficiency.

Systems	Year	PCE (%)	AVT (%)	Top electrode	Ref
<b>P3HT:PC<sub>61</sub>BM</b>	2017	2.9	24.7	Au/Ag Electrodes	6
		3.2	19.0	Dielectric Mirrors Electrodes	
<b>PTB7:PC<sub>71</sub>BM</b>	2017	5.5	34.1	Au/Ag Electrodes	
		6.4	16.9	Dielectric Mirrors Electrodes	
<b>PTB7-Th:PC<sub>71</sub>BM</b>	2017	5.4	27.6	Au/Ag Electrodes	
		7.0	12.2	Dielectric Mirrors Electrodes	
		6.4	11.5	Au/Ag Electrodes	
<b>PTB7-Th:FNIC1</b>	2018	9.14	14.7	Ag Electrodes	7
<b>PTB7-Th:FNIC2</b>		11.6	13.9		
<b>PTB7-Th:Coi8DFIC</b>	2018	6.17	23.99	Ag Electrodes	8
<b>PTB7-Th:Coi8DFIC:IEICO-4F</b>		9.37	17.23		
<b>PTB7-Th:IEICO-4F</b>	2019	8.35	25.3	Au/Ag Electrodes	9
<b>PTB7-Th:PC<sub>71</sub>BM</b>	2019	8.81	21.8	Photonic Crystals Electrodes	10
		8.65	25		
<b>PTB7-Th:IEICO-4F</b>	2019	10.97	20.6		
		11.25	21.5		
<b>J71:IHIC</b>	2019	8.26	28.1	Dielectric Mirrors Electrodes	11
		8.48	21.5		
<b>J71:PTB7-Th:IHIC</b>	2019	8.93	25.8	Dielectric Mirrors Electrodes	
		9.37	21.4		
<b>PBDB-T:PTB7-Th:IHIC</b>		8.33	27.5	Flexible	
		8.76	20.6	Dielectric Mirrors Electrodes	
<b>PM6:Y6</b>	2020	12.37	18.6	Au/Ag Electrodes	12
<b>PBT1-C-2Cl:Y6</b>	2020	11.7	19.7	Au/Ag Electrodes	13
<b>PBDB-T-2F:Y6</b>	2020	12.59	17	Ag Electrodes	14
<b>PTB7-Th:Coi8DFIC:PC<sub>61</sub>BM</b>	2020	10.68	12.54	30nm Ag	This Work
		10.27	16.15	20nm Ag	

**Table S3** Device parameters of the studied organic solar cells with different types of top electrodes.

Area (cm <sup>2</sup> )	Top electrode	V <sub>oc</sub> (V)	J <sub>sc</sub> (mA/cm <sup>2</sup> )	FF (%)	PCE (%)	AVT (%)	AVT loss	PCE gain
<b>1.25</b>	20 nm	0.67	21.52	55.84	8.05	16.49	—	—
<b>1.25</b>	20nm + Busbar 1	0.68	21.17	57.18	8.23	13.75	17.6%	1.02
<b>1.25</b>	20nm + Busbar 2	0.70	20.43	56.65	8.10	15.85	3.8%	1.006
<b>1.25</b>	15 nm	0.67	18.91	52.65	6.67	21.36	—	—
<b>1.25</b>	15 nm + Busbar 1	0.68	21.39	55.41	8.06	15.84	25.8%	1.20
<b>1.25</b>	15 nm + Busbar 2	0.68	20.84	54.62	7.74	18.27	14%	1.16
<b>1.25</b>	15 nm + Busbar 3	0.68	19.51	52.77	7.00	20.84	2.4%	1.04
<b>1.25</b>	15 nm + Busbar 4	0.68	19.25	54.48	7.13	20.43	4.3%	1.06
<b>1.25</b>	10 nm	0.67	7.43	23.51	1.17	25.14	—	—
<b>1.25</b>	10 nm + Busbar 3	0.68	14.83	35.00	3.53	23.71	5.68%	3.01
<b>1.25</b>	10 nm + Busbar 4	0.68	15.80	38.07	4.09	22.67	9.82%	3.49

#### Bottom electrode:

There are three steps for fabrication of bottom electrode. First of all, by blading the UV glue was deposited on top of glass substrate, and then was processed to designed pattern by photolithography. Through the patterned UV films, a Ni master plate was then fabricated as a mask. Patterning the PET substrate was the second step: blading the UV glue on the top of the PET substrate, and then forming a mask-like pattern on PET by embossing the nickel master on top of the UV glue. Finally, the Ag nanoink was filled into the groove by blading, and then sintered at 150°C for 15 min.

#### Top electrode:

The four types of UTMF+Busbar were fabricated by a template which was obtained by laser cutting technology with an industrial compatible laser equipment (USA Newport Laser μFAB / Spirit ps 1040-10 ). The laser cutting process is shown in Figure S4 c and d. Then, the template is placed on the top of the UTMF as a mask.

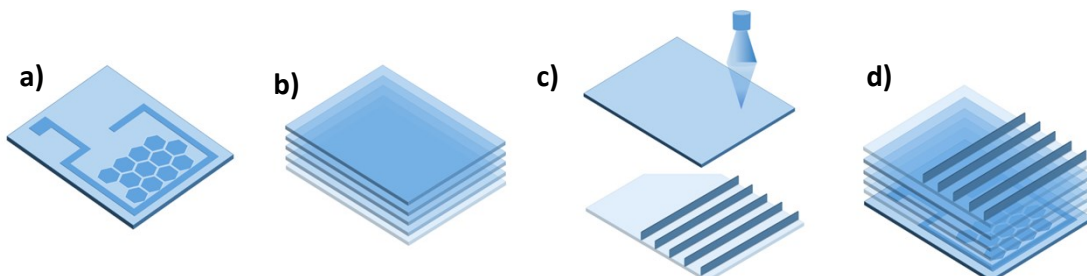


**Figure S1** Large-area flexible semitransparent organic solar cells fabrication process and diagram of laser assist grids integration process.

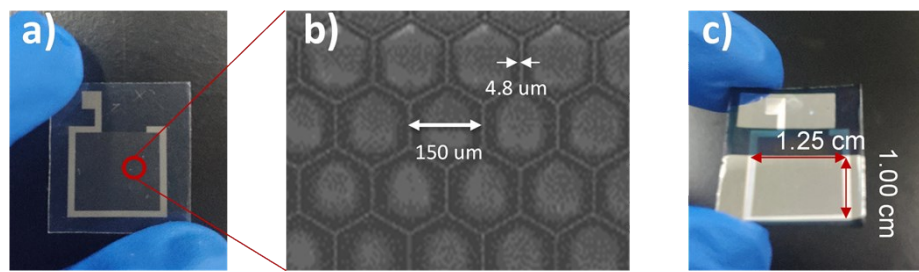


**Figure S2** Diagram of BFTE. (a) photo of our high transparency BFTE (b) Vapor-deposited large-area flexible semitransparent device photo, its effective area is  $1.25 \text{ cm}^2$ . (c) Optical microscopy and SEM images of the Ag silver grids substrate. (d) In the area of hexagonal meshes, hexagon silver grids connected like a honeycomb structure.

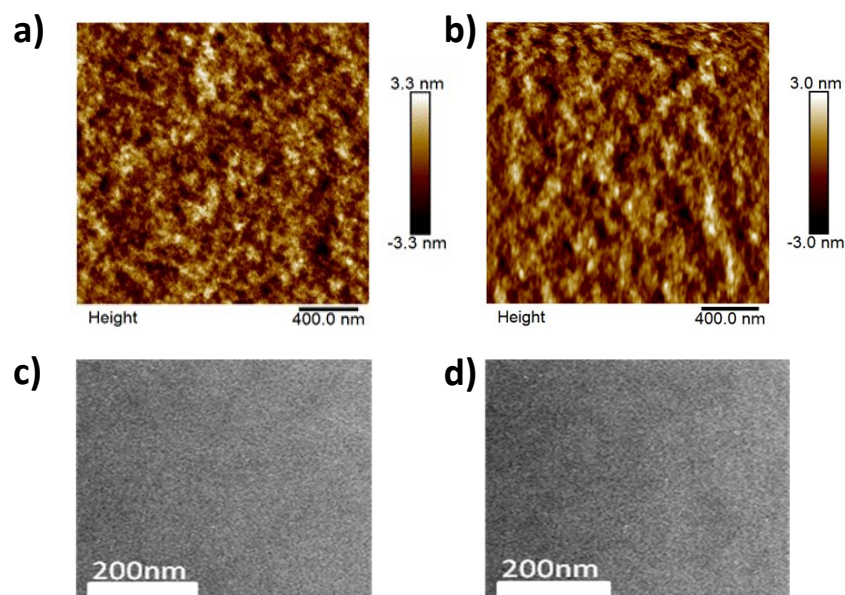


**Figure S3** AFM and TEM images of active layer fabricated with PET/ITO (a, c) and PET/silver grid (b, d) substrate.

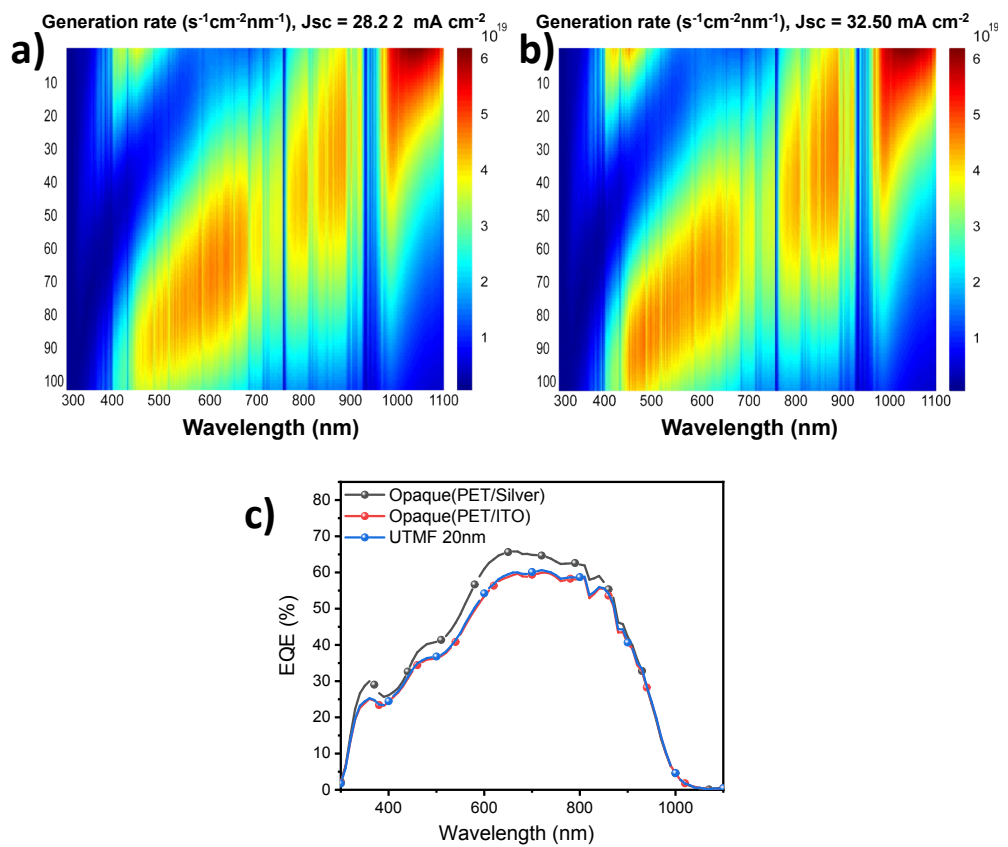


**Figure S4** (a-b) Exciton generation rate of PET/Sliver grids substrate and PET/ITO substrate devices. (c) EQE curves of large-area flexible opaque organic solar cells and large-area flexible semi-transparent organic solar cells.

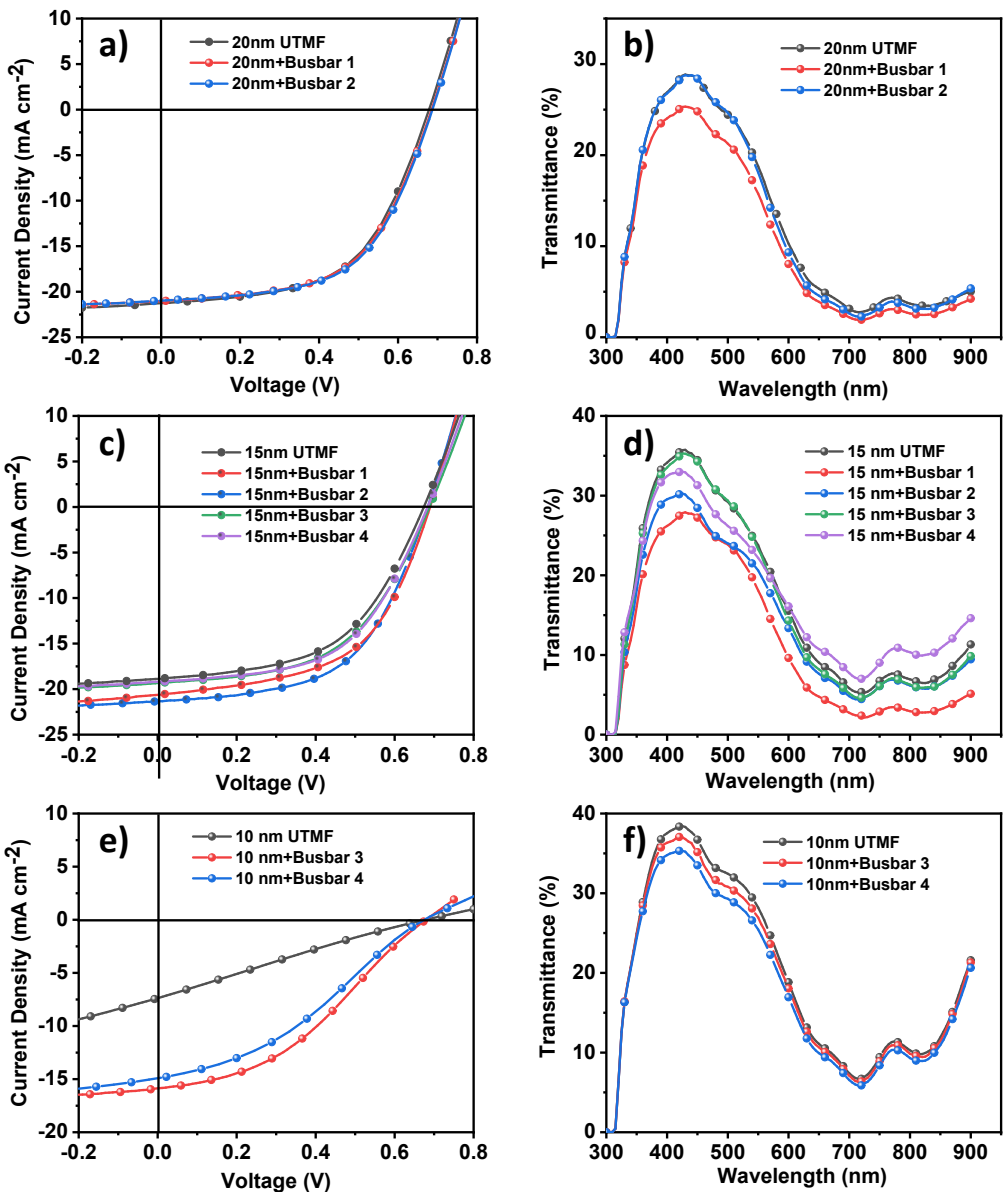


**Figure S5** The J-V curves and transmittance of different flexible large-area semitransparent devices.

## Reference

1. X. Li, H. Meng, F. Shen, D. Su, S. Huo, J. Shan, J. Huang and C. Zhan, Semitransparent fullerene-free polymer solar cell with 44% avt and 7% efficiency based on a new chlorinated small molecule acceptor, *Dyes and Pigments*, 2019, 166, 196-202.
2. E. Pascual-San-José, G. Sadoughi, L. Lucera, M. Stella, E. Martínez-Ferrero, G. E. Morse, M. Campoy-Quiles and I. Burgués-Ceballos, Towards photovoltaic windows: Scalable fabrication of semitransparent modules based on non-fullerene acceptors via laser-patterning, *J. Mater. Chem. A*, 2020, 8, 9882-9895.
3. L. Zuo, S. Zhang, M. Shi, H. Li and H. Chen, Design of charge transporting grids for efficient ito-free flexible up-scaled organic photovoltaics, *Mater. Chem. Front.*, 2017, 1, 304-309.
4. J. Czolk, D. Landerer, M. Koppitz, D. Nass and A. Colsmann, Highly efficient, mechanically flexible, semi-transparent organic solar cells doctor bladed from non-halogenated solvents, *Adv. Mater.*

Technol., 2016, 1, 1600184.

5. J. Huang, C. Z. Li, C. C. Chueh, S. Q. Liu, J. S. Yu and A. K. Y. Jen, 10.4% power conversion efficiency of ito-free organic photovoltaics through enhanced light trapping configuration, *Adv. Energy. Mater.*, 2015, 5, 1500406.
6. G. Y. Xu, L. Shen, C. H. Cui, S. P. Wen, R. M. Xue, W. J. Chen, H. Y. Chen, J. W. Zhang, H. K. Li, Y. W. Li and Y. F. Li, High-performance colorful semitransparent polymer solar cells with ultrathin hybrid-metal electrodes and fine-tuned dielectric mirrors, *Adv. Funct. Mater.*, 2017, 27, 1605908.
7. J. Wang, J. Zhang, Y. Xiao, T. Xiao, R. Zhu, C. Yan, Y. Fu, G. Lu, X. Lu, S. R. Marder and X. Zhan, Effect of isomerization on high-performance nonfullerene electron acceptors, *J. Am. Chem. Soc.*, 2018, 140, 9140-9147.
8. X. Ma, Z. Xiao, Q. An, M. Zhang, Z. Hu, J. Wang, L. Ding and F. Zhang, Simultaneously improved efficiency and average visible transmittance of semitransparent polymer solar cells with two ultra-narrow bandgap nonfullerene acceptors, *J. Mater. Chem. A*, 2018, 6, 21485-21492.
9. Z. Hu, J. Wang, Z. Wang, W. Gao, Q. An, M. Zhang, X. Ma, J. Wang, J. Miao, C. Yang and F. Zhang, Semitransparent ternary nonfullerene polymer solar cells exhibiting 9.40% efficiency and 24.6% average visible transmittance, *Nano Energy*, 2019, 55, 424-432.
10. R. X. Xia, C. J. Brabec, H. L. Yip and Y. Cao, High-throughput optical screening for efficient semitransparent organic solar cells, *Joule*, 2019, 3, 2241-2254.
11. Y. W. Li, G. Y. Xu, C. H. Cui and Y. F. Li, Flexible and semitransparent organic solar cells, *Adv. Energy. Mater.*, 2018, 8, 1701791.
12. Z. Hu, Z. Wang, Q. An and F. Zhang, Semitransparent polymer solar cells with 12.37% efficiency and 18.6% average visible transmittance, *Science Bulletin*, 2020, 65, 131-137.
13. Y. P. Xie, Y. H. Cai, L. Zhu, R. X. Xia, L. L. Ye, X. Feng, H. L. Yip, F. Liu, G. H. Lu, S. T. Tan and Y. M. Sun, Fibril network strategy enables high-performance semitransparent organic solar cells, *Adv. Funct. Mater.*, 2020, 30, 2002181.
14. W. Song, B. Fanady, R. X. Peng, L. Hong, L. R. Wu, W. X. Zhang, T. T. Yan, T. Wu, S. H. Chen and Z. Y. Ge, Foldable semitransparent organic solar cells for photovoltaic and photosynthesis, *Adv. Energy. Mater.*, 2020, 10, 2000136.